



Surface Crack Characterization of Aluminium Specimen using Passive Wireless RFID based Tag Antenna Sensor

Setti Suresh¹, and Geetha Chakaravarthi²

Applied Electromagnetics Laboratory, Department of Instrumentation and Control Engineering
National Institute of Technology, Trichy, India

settisuresh1@gmail.com¹

geethac@nitt.edu²

Abstract

This paper presents an Ultra High Frequency (UHF) Radio Frequency Identification (RFID) based tag antenna sensor for surface crack characterization of an aluminium alloy 6061 T6 grade specimen. Tag antenna was optimised using HFSS®, Ansys Inc., USA software. The designed tag is simulated on the specimen with various crack dimensions and orientations. When the crack depth is varied from 0 to 1 mm, the observed average absolute change in resonant frequency ($|\Delta f_r|$) for vertical, horizontal, and diagonal orientation cracks is 2.19 MHz, 0.39 MHz, and 1.05 MHz, respectively. Similarly, for varying crack depths from 1mm to 6mm, the observed frequencies are 10.21 MHz, 0.6 MHz, and 4.5 MHz, respectively. Simulation results show that the proposed sensor is sensitive to submillimeter cracks, enabling the detection of surface cracks at an early stage.

Index Terms – Metallic surface cracks, Microstrip Antenna, RFID Sensor, Structural Health Monitoring

1. Introduction

Structural Health Monitoring (SHM) of large-scale infrastructure is a continuous task to be performed for early detection of impending cracks, ensuring structural integrity and extending the service life of structures [1]. Addressing the above concern, there are several conventional NDE approaches using radiography, ultrasonic, eddy current, magnetic particle, and penetrant testing, which are tedious and time-consuming. The measures are costly, as the inspection is labor-intensive and extensive sample preparation is often required [2]. On the contrary, the application of passive wireless RFID sensors for pervasive surface crack monitoring [3] is an emerging area of interest due to its benefits like unique identification, passive wireless monitoring, and mass production of sensors at a very low cost.

The literature [4] study reveals that there are several RFID based crack sensors that can detect surface cracks of mm resolution with different dimensions and orientations. A 3D antenna based UHF RFID sensor system for the progressive surface crack characterization of an aluminium specimen has been presented for varying crack

depths at mm resolution [5]. The increasing crack depth is depicted in terms of a shift in frequency and quantified using a kernel PCA-based feature extraction method. Later, the aluminium specimen with the same crack dimensions was tested with a commercial RFID tag to make low-cost RFID sensing more reliable [6]. Some RFID crack sensors in the literature are sensitive to longitudinal cracks with varying crack depths [7] and varying lengths [8] at mm-resolution. Though there are several designs for surface crack characterization on metallic structures, the study lacks the analysis of submillimeter (sub-mm) cracks, with different crack dimensions and orientations. Hence, a new tag design has been proposed to investigate the surface cracks on an aluminium specimen, where the material of interest is most commonly used in safety-critical applications like aerospace [9] and ship structures [10].

The paper is organised as follows: Methodology, describing the tag antenna sensor design and crack characterization mechanism, is presented in Section 2. The results and discussion of the simulated design are explained in Section 3, and finally, Section 4 concludes the paper.

2. Methodology

2.1 Tag Antenna Design

The numerical model of the RFID tag antenna sensor was designed using Finite Element Method (FEM) based 3D electromagnetic simulation software. Fig. 1 (a) shows the designed tag placed on a numerical aluminium specimen model of dimensions $(400 \times 100 \times 10)$ mm³ with simulated surface cracks at different crack depths. The tag antenna was realised on a standard two-layer Rogers RO3010 substrate material formed to a thickness of 1.902 mm, with upper and lower bonding layer thicknesses of 0.632 mm and 1.27 mm, respectively, with a dielectric constant (ϵ_r) of 11.2 and a dissipation factor ($\tan\delta$) of 0.0022. The top copper layer is of thickness 55 μ m, together with the substrate, leading to a tag thickness of 1.957mm as shown in Fig. 1(b). Designed tag antenna parameters with all dimensions is shown in Fig. 2 (a). To induce a high amount of current on the metal surface, two rectangular patches of dimension $(17 \times 12 \times 0.055)$ mm³ and two feed path strips of dimension $(12 \times 3.25 \times 0.055)$ mm³ have been used in the antenna design. The design is optimised to an overall

dimension of $(44 \times 44 \times 1.957)$ mm³ operating in the frequency region (860-960) MHz. The fabricated RFID tag antenna sensor soldered with Alien Technologies Higgs-4 RFID IC is shown in Fig. 2 (b). For No Crack (NC) specimen, the tag resonates at a frequency of 915.3 MHz with a negative gain of 2.835 dB as shown in Fig. 3.

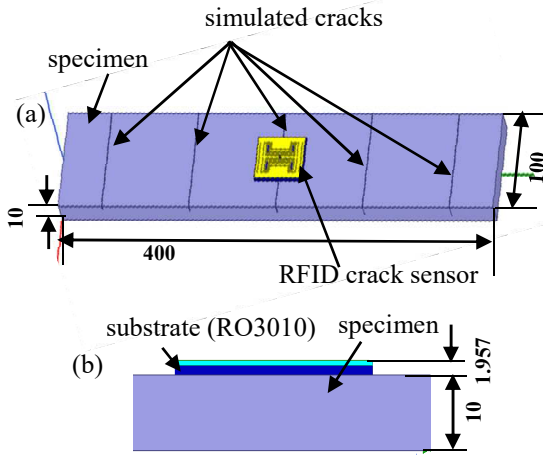


Figure 1. Numerical model of RFID Tag antenna sensor placed on specimen with simulated cracks (a) Top view (b) Side view ; Note: dimensions are in mm

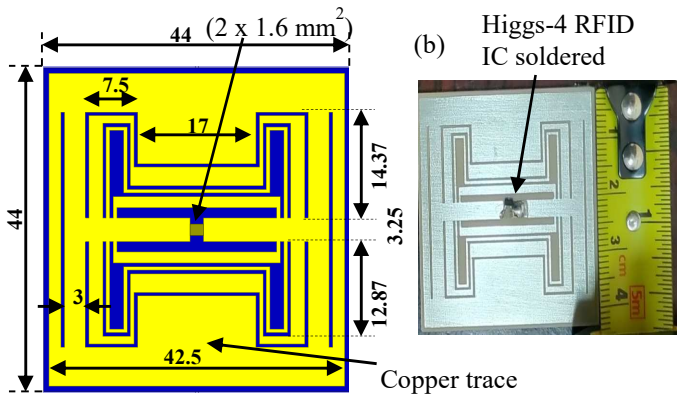


Figure 2. Designed tag with dimensions in mm (a) Simulation (b) Fabricated tag.

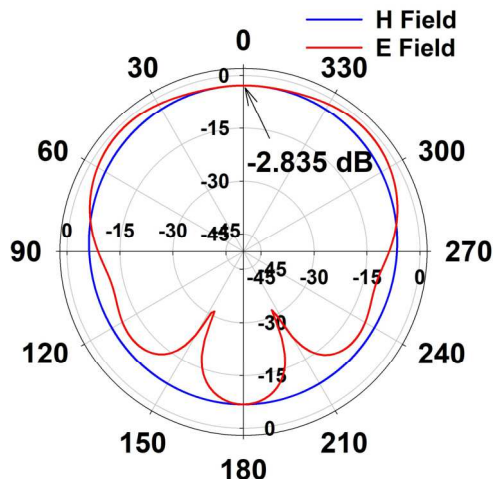


Figure 3. Simulated tag gain plot at 915 MHz

2.2 Crack Characterization Mechanism

Fig. 4 shows the induced surface current distribution on the specimen for different crack orientations. It is observed that the surface current distribution is greater in the vicinity of the feed path strips. When a vertical crack is induced in the specimen surface, it has a large-scale effect on the flow of surface current distribution, as shown in Fig. 4(a). The resonant frequency relation with respect to the change in surface current length [11] on the metal specimen is given by equation:

$$f_r = \frac{c}{2\sqrt{\epsilon_{r,eff}}} \cdot \frac{1}{L + \Delta L} \quad (1)$$

Where f_r is resonant frequency of tag, c is speed of light in free space, $\epsilon_{r,eff}$ is effective dielectric constant, L is physical length of patch and ΔL is the additional electrical length due to fringing effect.

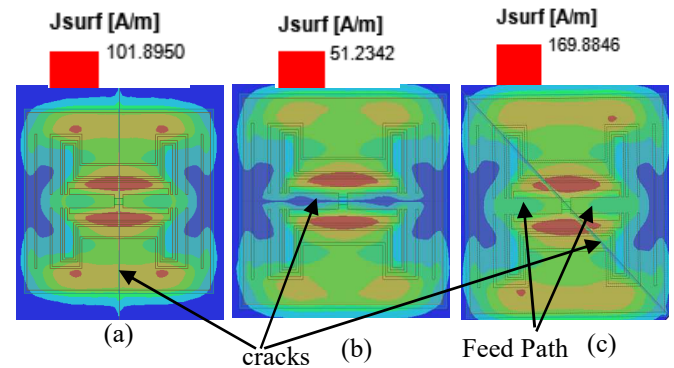


Figure 4. Simulated surface current distribution on the specimen for different crack orientations (a) Vertical (b) Horizontal (c) Diagonal

From equation (1), it can be inferred that resonant frequency is inversely proportional to the change in surface current length on the metal specimen. Both in vertical and diagonal orientations, as the crack depth increases, the length of induced surface current travels also increases, resulting in decreased resonant frequency. The presence of vertical and diagonal crack disturbing the flow of surface current on the specimen is shown in Figs. 4(a) and 4(c), where vertical crack is having a greater effect on the tag surface current distribution than diagonal crack. However, in the case of a horizontal orientation, the crack propagation has minimal effect on the surface current distribution, as shown in Fig 4 (b).

3. Results and Discussion

The simulation study of sub-mm and mm cracks with three different crack orientations on the aluminium specimen and the tag response in terms of frequency shift is discussed in this section. To study the tag response for varying crack depths in sub-mm and mm resolution, the length and width of crack are kept constant at 100mm and 0.5mm. Fig. 5 (a) shows the observed shift in resonant frequency from 915.3

MHz to 911.55 MHz for varying crack depth from 0 to 1mm with a step size of 0.2mm in vertical orientation. It indicates that the f_r is shifting towards left i.e., decreasing from its NC f_r . Further for mm resolution, varying the crack depth from 1mm to 6mm with a step size of 1mm, it is observed that the f_r is shifting towards left with an increased rate of change in frequency as shown in Fig. 5(b). Similarly, for horizontal and diagonal orientation sub-mm and mm resolution cracks, the shift in f_r is observed as shown in Figs. 5(c), 5(d) and 5(e), 5(f), respectively. It can be inferred that the f_r is shifting towards right, i.e., increasing for horizontal orientation but with lesser frequency shift as discussed in Section 2.2. To quantify the orientation of crack with varying crack depths, the change in resonant frequency from NC to With Crack (WC) is calculated using the following equation:

$$\Delta f_r = f_r(NC) - f_r(WC) \quad (2)$$

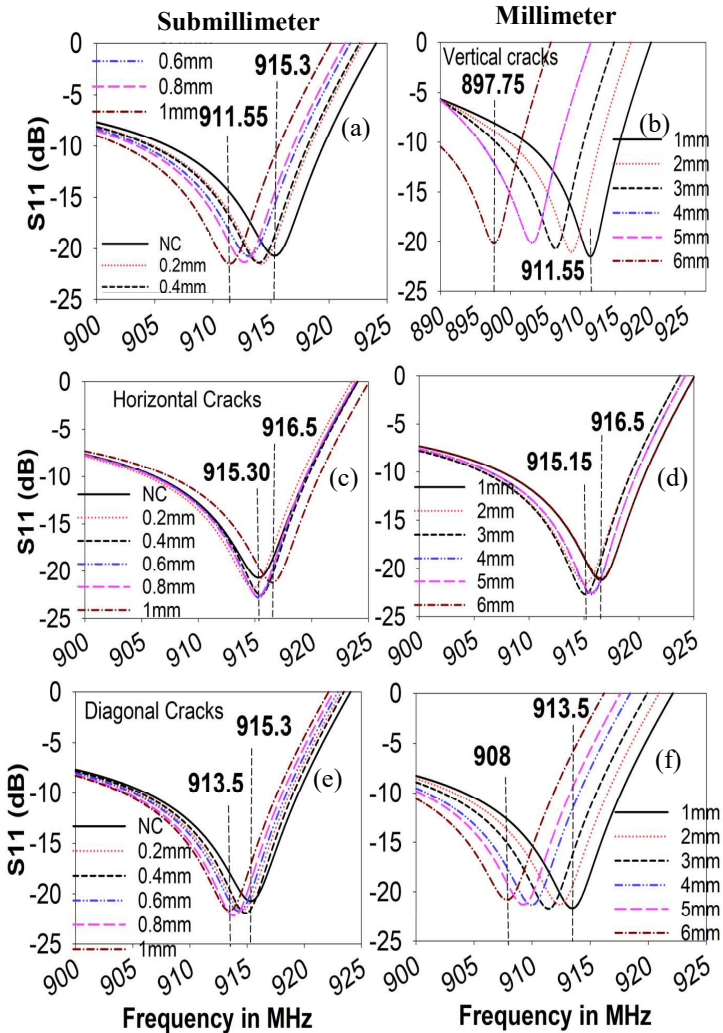


Figure 5. Simulated return loss for crack dimensions of length – 100 mm, width – 0.5 mm and depth varying for (a) vertical sub-mm (b) vertical mm (c) horizontal sub-mm (d) horizontal mm (e) diagonal sub-mm (f) diagonal mm - resolution cracks.

From eq. (2), Δf_r is calculated for all the crack cases and the average absolute change in resonant frequency ($|\Delta f_r|$) for vertical (V), horizontal (H), and diagonal (D) crack orientations with sub-mm resolution are observed to be 2.19, 0.39, and 1.05, respectively. Fig. 6 shows the resonance frequency response for varying crack depths for both sub – mm and mm resolution. From Fig. 6 (a), it can be inferred that the $|\Delta f_r|$ is decreasing for both vertical and diagonal crack orientations but with a different slope. For horizontal crack orientation, it is observed to be an increasing behavior. Similarly, for mm resolution, the behavior is same with increased $|\Delta f_r|$ rate as shown in Fig. 6 (b). Table 1 shows the calculated average $|\Delta f_r|$ for varying cracks depths and for mm resolution, it is observed to be 10.21, 0.6 and 4.5 for corresponding vertical, horizontal and diagonal crack orientations. The $|\Delta f_r|$ behavior for varying crack width from 0.2 mm to 1 mm with a step size of 0.2mm, keeping depth and length constant at 1mm and 100mm is also presented in Table 1, where the $|\Delta f_r|$ rate is different from varying crack depths. The above simulation study shows that the proposed RFID tag antenna sensor is sensitive to sub-mm and mm resolution cracks with different orientations.

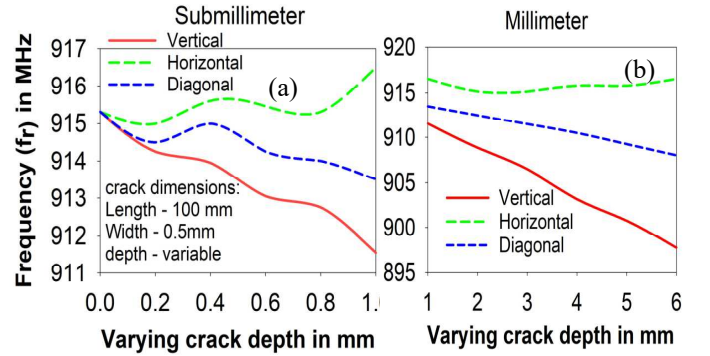


Figure 6. Resonant frequency response with respect to crack propagation (a) sub-mm and (b) mm resolutions

Table 1. Average absolute change in f_r for different crack orientations

Crack dimensions		Average $ \Delta f_r $ in MHz		
		V	H	D
Varying depth	Sub-mm	2.19	0.39	1.05
	mm	10.21	0.6	4.5
Varying width	Sub-mm	3.85	0.84	1.65

4. Conclusion and Future Work

This work presents the design of an RFID based tag antenna sensor for surface crack characterization on aluminium alloy specimen with sub-mm cracks. The crack growth is studied in three different orientations and the simulated analysis shows that the tag is able to detect the sub-mm and mm resolution cracks with differential shift in resonant frequency response. It is observed that, the tag is highly sensitive to vertical orientation cracks followed by diagonal and horizontal cracks with varying crack depth

from 0 to 1mm and 1mm to 6mm. The tag is also effective for varying crack width characterization for different orientations in sub-mm resolution. As the tag is having unique identification, it can be used for localization of crack on a larger structure by positioning the sensor at different stress locations. Experimental validation with the fabricated sensor on the aluminium specimen with artificially induced cracks will be carried out and the feasibility of automatic surface crack characterization will be investigated.

5. Acknowledgment

The authors would like to thank the SERB (SRG/2019/001397), a statutory body of the Department of Science & Technology, Government of India, for supporting this research and Alien Technology, LLC, USA, for providing free RFID IC samples.

6. References

- [1] C. R. Farrar and K. Worden, "An introduction to structural health monitoring," *Philos. Trans. R. Soc. A Math. Phys. Eng. Sci.*, vol. 365, no. 1851, pp. 303–315, Dec. 2006, doi: 10.1098/RSTA.2006.1928.
- [2] P. Cawley, "Non-destructive testing—current capabilities and future directions:," <http://dx.doi.org/10.1177/146442070121500403>, vol. 215, no. 4, pp. 213–223, Aug. 2016, doi: 10.1177/146442070121500403.
- [3] P. Kalansuriya, R. Bhattacharyya, and S. Sarma, "RFID tag antenna-based sensing for pervasive surface crack detection," *IEEE Sens. J.*, vol. 13, no. 5, pp. 1564–1570, 2013, doi: 10.1109/JSEN.2013.2240155.
- [4] S. Suresh and G. Chakaravarthi, "RFID technology and its diverse applications: A brief exposition with a proposed Machine Learning approach," *Measurement*, vol. 195, p. 111197, May 2022, doi: 10.1016/J.MEASUREMENT.2022.111197.
- [5] J. Zhang, G. Y. Tian, and A. B. Zhao, "Passive RFID sensor systems for crack detection & characterization," *NDT E Int.*, vol. 86, pp. 89–99, Mar. 2017, doi: 10.1016/J.NDTEINT.2016.11.002.
- [6] J. Zhang, A. I. Sunny, G. Zhang, and G. Tian, "Feature extraction for robust crack monitoring using passive wireless RFID antenna sensors," *IEEE Sens. J.*, vol. 18, no. 15, pp. 6273–6280, Aug. 2018, doi: 10.1109/JSEN.2018.2844564.
- [7] J. Zhang, B. Huang, G. Zhang, and G. Y. Tian, "Wireless Passive Ultra High Frequency RFID Antenna Sensor for Surface Crack Monitoring and Quantitative Analysis," *Sensors 2018, Vol. 18, Page 2130*, vol. 18, no. 7, p. 2130, Jul. 2018, doi: 10.3390/S18072130.
- [8] Y. Xu, L. Dong, H. Wang, X. Xie, and P. Wang, "Surface crack detection and monitoring in metal structure using RFID tag," *Sens. Rev.*, vol. 40, no. 1, pp. 81–88, Mar. 2020, doi: 10.1108/SR-06-2019-0153.
- [9] P. Rambabu, N. Eswara Prasad, V. V. Kutumbarao, and R. J. H. Wanhill, "Aluminium Alloys for Aerospace Applications," pp. 29–52, 2017, doi: 10.1007/978-981-10-2134-3_2.
- [10] E. Thomas, "Aluminum Ship Structures."
- [11] Z. Liu, K. Chen, Z. Li, and X. Jiang, "Crack Monitoring Method for an FRP-Strengthened Steel Structure Based on an Antenna Sensor," *Sensors 2017, Vol. 17, Page 2394*, vol. 17, no. 10, p. 2394, Oct. 2017, doi: 10.3390/S17102394.